A Generalized Model to Estimate Reaction Time Corresponding to Visual Stimulus Using Single-Trial EEG

Mohammad Samin Nur Chowdhury[1*], Arindam Dutta[1], Matthew K. Robison[2], Chris Blais[2], Gene Brewer[2], and Daniel W. Bliss[1]

***Abstract*— The estimation of the visual stimulus-based reaction time (RT) using subtle and complex information from the brain signals is still a challenge, as the behavioral response during perceptual decision making varies inordinately across trials. Several investigations have tried to formulate the estimation based on electroencephalogram (EEG) signals. However, these studies are subject-specific and limited to regression-based analysis. In this paper, for the first time to our knowledge, a generalized model is introduced to estimate RT using single-trial EEG features for a simple visual reaction task, considering both regression and classification-based approaches. With the regression-based approach, we could predict RT with a root mean square error of 111.2 ms and a correlation coefficient of 0.74. A binary and a 3-class classifier model were trained, based on the magnitude of RT, for the classification approach. Accuracy of 79% and 72% were achieved for the binary and the 3-class classification, respectively. Limiting our study to only high and low RT groups, the model classified the two groups with an accuracy of 95%. Relevant EEG channels were evaluated to localize the part of the brain significantly responsible for RT estimation, followed by the isolation of important features.**

***Clinical relevance*— Electroencephalogram (EEG) signals can be used in Brain-computer interfaces (BCIs), enabling people with neuromuscular disorders like brainstem stroke, amyotrophic lateral sclerosis, and spinal cord injury to communicate with assistive devices. However, advancements regarding EEG signal analysis and interpretation are far from adequate, and this study is a step forward.**

I. INTRODUCTION

The human brain controls a person's actions/reactions, and response to a particular event directly depends on the type of stimulus and the brain functionalities. A lot of previous psychological experiments on human behavior have been conducted to understand human reactions in terms of brain activities [1]. However, as the brain is one of the largest and most complicated parts of the human body with uncountable functions, there is a long way to go to unfold all the mysteries. This paper concentrates on the human reaction towards visual stimulus and tries to estimate reaction time (RT) from information embedded in electroencephalogram (EEG) signals.

A recent study [2] demonstrated a method to estimate RT based on Riemannian tangent space features from EEG data taken from 16 participants. Another investigation [3] tried to estimate the timing of target onset during rapid serial visual presentation based on single-trial EEG using data from 6 subjects. There are other similar studies, and all of them employ subject-specific, regression-only estimation models. This study tries to overcome the existing limitations by proposing a feature extraction-based generalized model that uses single-trial EEG data. Also, it takes into account a classification approach aside from regression. The study incorporates multi-domain feature extraction from different EEG channels [4] to feed machine learning models for the RT estimation. Furthermore, it discusses methods for essential channels (brain locations) and features isolation.

II. METHODS

A. Experiment Details

A total of 48 participants (31 males, 17 females) of ages ranging from 18 to 24 performed a simple visual reaction task. The experimental setup can be explained as follows. In a computer screen, a plus symbol (+) appears at the center, and after variable time duration, the symbol changes into a cross ($\times$). The task of every subject is to tap the space bar as soon as the symbol changes from plus (+) to cross ($\times$). This action is repeated several times for each subject, and every single repetition is considered as a trial. For each subject, the duration of the experiment was about 30 minutes, and the average number of trials was around 320. During the entire experiment, noninvasive scalp EEG signals from 30 effective channels were recorded for all the participants. The subjects had normal or corrected to normal vision with no history of neurological problems, and informed consent was obtained from each of them. The Institutional Review Board of Arizona State University approved all the procedures.

B. Data Handling and Preprocessing

The data had a sampling rate of 1kHz and were filtered from DC to 400 Hz to get rid of the high-frequency noise. The ocular artifacts were removed by visual inspection of the ocular components obtained from independent component analysis (ICA). Afterward, the data were normalized by mean and variance. In the EEG data, there was a pair of starting and ending point indicators for each subject. The following events repeated several times sequentially between them depending on the number of trials:

1) beginning of the trial (+)
2) change of symbol ($\times$)
3) response of the subject (space bar tap)

This work was not supported by any organization

[1] M. S. N. Chowdhury, A. Dutta, and D. W. Bliss are with School of Electrical, Computer & Energy Engineering, Arizona State University

[2] M. K. Robison, C. Blais, and G. Brewer are with Dpt. of Psychology, Arizona State University

* Corresponding author email: mchowd12@asu.edu

978-1-7281-1990-8/20/$31.00 ©2020 IEEE

The observation sequence is the multi-channel EEG signal between 1 and 2, and the RT is the time between 2 and 3. For every trial, we segmented and stored the observation sequence and the RT of the subject. RTs above 1000ms were extremely rare and can be considered as exceptions. Those RTs and the corresponding observation sequences were excluded from the dataset.

C. Feature Extraction

A total of 55 features from time, frequency, and time-frequency domain were extracted for each channel.

1) Time Domain Features: Time-domain observation sequences with lengths ranging from 919 ms to 8908 ms were used to measure average power and Hjorth parameters [5] as temporal features.

The average power was calculated by computing the total energy and dividing it by the time duration. On the other hand, Hjorth parameters (activity, mobility, complexity) were calculated using equation (1), (2), and (3), respectively.

$$activity = var\big(y(t)\big) \tag{1}$$

$$mobility = \sqrt{\frac{var\big(\frac{dy(t)}{dt}\big)}{var\big(y(t)\big)}} \tag{2}$$

$$complexity = \frac{Mobility\big(\frac{dy(t)}{dt}\big)}{Mobility\big(y(t)\big)} \tag{3}$$

where $y(t)$ is the EEG signal from any channel corresponding to an observation sequence, and var indicates variance.

2) Frequency Domain Features: The spectral representation obtained using the fast Fourier transform (FFT) provided us with spectral entropy and frequency band-based features.

Spectral entropy (SEN) is the normalized Shannon entropy, applied to the power spectrum density of the EEG signal [6]. SEN can be calculated using equation (4).

$$SEN = \frac{-\sum P_k \log P_k}{\log N} \tag{4}$$

where P_k are the spectral powers of the normalized frequencies such that $\sum P_k = 1$, and N is the number of frequencies (bin).

The EEG frequency domain sequence can be divided into five bands based on frequency, namely delta (1-4Hz), theta (4-8Hz), alpha (8-12Hz), beta (12-35Hz), and gamma (35-150Hz). These bands are carriers of event-related information [7], and following band-specific features were extracted:

1) percentage of energy in each frequency band
2) inter-band power ratios ($\delta/\theta, \theta/\alpha, \alpha/\beta$, and β/γ)
3) maximum, minimum, and median value of 1 and 2 for multiple non-overlapping 0.1 seconds long rectangular windows across the whole observation sequence

3) Time-Frequency Domain Features: Time-frequency domain representation was obtained using the reassigned version of the spectrogram, which can be calculated using equation (5).

$$S_x(m,\omega) = \left| \sum_{n=-\infty}^{\infty} x[n]h[n-m]e^{-j\omega n} \right|^2 \tag{5}$$

where $x[n]$ is the signal, and $h[n]$ is the window function. We used the Hamming window for our calculation. From time-frequency domain representation, Renyi information and ridge based features were extracted.

Renyi information reveals a signal's complexity indicating the number of basic sinusoids involved in it [8]. Equation (6) presents the mathematical expression for the calculation of Renyi information.

$$R_x^\alpha = \frac{1}{1-\alpha} \log_2 \left[\sum_{m=-\infty}^{\infty} \sum_{\omega=-\infty}^{\infty} S_x^\alpha(m,\omega) \right] \tag{6}$$

where R_x^α is the Renyi information of order α, and for our calculation, we used $\alpha = 3$.

Ridge plot provides the location of the peaks in the time-frequency representation. We obtained it using the MATLAB-based time-frequency toolbox. The average number of ridges across the time for each frequency band was taken as a feature.

4) Last Moment Observation Effect: To see if the last moment observation has any impact on the outcome, all the stated features were extracted again from just the final 0.8 seconds of the observation period, instead of the whole observation.

D. Regression

Using extracted features, the regression-based analysis was performed to estimate RT. The following regression models were considered and trained in this study:

1) Linear Regression
2) Ridge Regression
3) Support Vector Regression with Radial Basis Function (RBF) Kernel
4) Random Forest Regression
5) Extra Tree Regression

Before implementing the algorithms, the dataset was adequately balanced, randomized, and segmented into training (80%) and testing (20%) sets. This ratio ensured low variance for both training parameter estimates and testing performance statistics to provide steady performance.

E. Classification

Splitting the RTs into different categories, we formulated a classification-based study on the existing dataset. It can be particularly helpful in cases where high-precision categorical grouping is required instead of the exact estimation.

A binary classification case was considered, where the data separation point was chosen as 500ms (midpoint of RT range) and the classes can be labeled as:

1) above midpoint (RT>500 ms)
2) below midpoint (RT<=500ms)

As mean RT is around 400 ms, a 3-class classification case was also formulated where the class boundaries were 400 $\pm$ 100 ms around. The classes can be labeled as:

1) low RT (RT<=315 ms)
2) medium RT (315ms<RT<=515ms)
3) high RT (RT>515ms)

As the number of data points was way too high in the medium RT class, class weight balance or training data balance was required, to perform 3-class classification.

Lastly, it is also of interest to see how well our method can discriminate between extremes. So, a binary classification was performed, excluding data from medium response class.

For all 3 types of classifications, the following classification models were considered:

1) Linear Regression
2) Support Vector Classifier (SVC) with RBF Kernel
3) Stochastic Gradient Descent (SGD) with SVC Model
4) Decision Tree
5) Random Forest

Though linear regression is not a classification algorithm, appropriate thresholding can transform the outcomes into desired class labels.

F. Important Channels and Features Isolation

We designed an algorithm for channel selection, that recursively eliminates unnecessary channels, preserving or enhancing the overall accuracy for binary classification of extremes. The logical implementation of the algorithm is demonstrated in Algorithm 1. Further, the outcomes of the algorithm were combined with tree-based feature importance method and mutual information-based feature selection criterion [9] for the best results.

A similar procedure was followed for the isolation of features. However, before that, a correlation matrix was formed to identify highly correlated (correlation coefficient > 0.75) features and clear out repetitions by eliminating the ones with a relatively lower correlation to the output labels.

Algorithm 1: Channel Isolation

Input: EEG features from all the channels
Output: useful channels
Initialization: $N \leftarrow 0$,
useful channels $\leftarrow$ {1,2,3,...,29,30}
while $N \neq$ *size of useful channels* **do**
  $N \leftarrow$ size of useful channels
  $X \leftarrow$ Random Forest accuracy for useful channels
  channels $\leftarrow$ null
  for $n \leftarrow$ *1 to N* **do**
    modified features $\leftarrow$ EEG features for (useful channels - n_{th} element of useful channels)
    accuracy $\leftarrow$ Random Forest accuracy using modified features
    if accuracy $>= X$ **then**
      $X \leftarrow$ accuracy
    else
      channels.append (n_{th} element of useful channels)
  useful channels $\leftarrow$ channels

TABLE I
REGRESSION-BASED ANALYSIS RESULTS

Algorithm	Correlation Coeff.	RMSE (ms)
Linear Regression	0.56	158.7
Ridge Regression	0.56	157.6
Support Vector Regression	0.60	136.7
Extra Tree Regression	0.73	114.4
Random Forest Regression	**0.74**	**111.2**

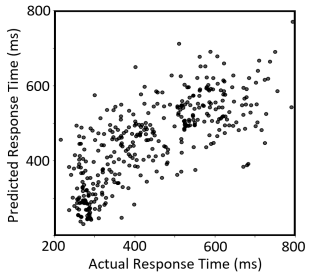

Fig. 1. Actual vs. predicted RT for the Random Forest model

III. RESULTS

A. Regression

Predictions higher than 1000ms were clipped to 1000ms. The root mean square error (RMSE) and correlation coefficient (CC) for each prediction are shown in Table 1. Clearly, the Random Forest model exhibited the best performance with an RMSE of 111.2 ms and a CC of 0.74. The actual vs. predicted RT for the testing set using the Random Forest model is shown in figure 1.

B. Classification

Tables 2, 3, and 4 discuss the accuracy, precision, & recall values for the classification-based analyses. The Random Forest model again outperformed all the others. Figure 2 shows the confusion matrix interpretations for the Random Forest model. The high accuracy (95%) obtained from the classification of extremes can be explained by the fine separation of classes 1 and 3 in the confusion matrix for 3-class classification.

TABLE II
BINARY CLASSIFICATION RESULTS FOR BELOW AND ABOVE MIDPOINT CATEGORIES

Algorithm	Accuracy (%)	Precision	Recall
Linear Regression	67	0.67	0.67
Decision Tree	63	0.63	0.63
SGD	63	0.63	0.63
SVM	73	0.72	0.73
Random Forest	**79**	**0.79**	**0.78**

TABLE III
3-CLASS CLASSIFICATION RESULTS FOR LOW, MEDIUM & HIGH RT

Algorithm	Accuracy (%)	Precision	Recall
Linear Regression	52	0.54	0.53
Decision Tree	56	0.55	0.56
SGD	59	0.56	0.56
SVM	70	0.54	0.59
Random Forest	**72**	**0.71**	**0.70**

TABLE IV

BINARY CLASSIFICATION RESULTS FOR HIGH AND LOW CATEGORIES

Algorithm	Accuracy (%)	Precision	Recall
Linear Regression	80	0.82	0.82
Decision Tree	85	0.84	0.86
SGD	80	0.78	0.79
SVM	85	0.85	0.83
Random Forest	**95**	**0.96**	**0.93**

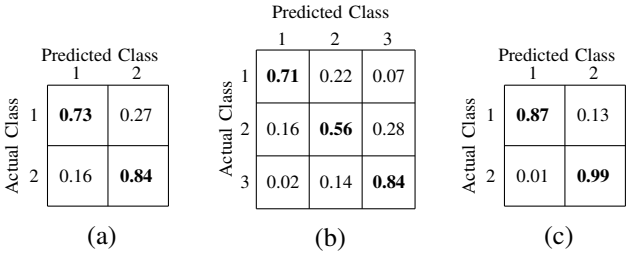

Fig. 2. Confusion matrix for (a) below/above midpoint-based binary classification, (b) 3-class classification, (c) high/low response-based binary classification

C. Important Channels and Features Isolation

Using the stated set of methods on the model with the best performance for the binary classification of extremes, it was found that T7, C3, TP7, CP3, P7, and P3 channels are of the highest importance. Figure 3 shows the relative importance of the EEG channels.

Eliminating the repetitions, we had 44 features for each channel. Among them, Hjorth parameters and power ratio-based features contributed the most in the estimation of RT. Furthermore, theta and alpha were the most dominant frequency bands. The top ten EEG features common to all the important channels are listed in Table 5.

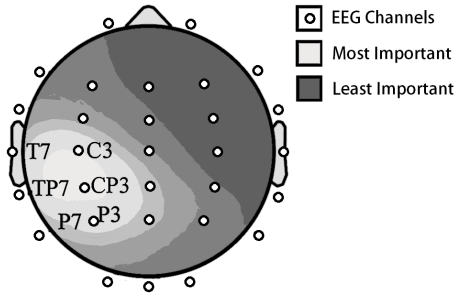

Fig. 3. Relative importance of the EEG channels

TABLE V

10 MOST IMPORTANT FEATURES AND CORRESPONDING WEIGHTS

Rank	Feature	Weight
1	Activity	0.0513
2	Activity of last moment	0.0413
3	Complexity	0.0363
4	Complexity of last moment	0.0335
5	Min. theta power/alpha power (moving windows)	0.0283
6	Mobility	0.0247
7	Med. theta power/alpha power (moving windows)	0.0234
8	Max. alpha energy percentage (moving windows)	0.0228
9	Min. delta power/theta power (moving windows)	0.0219
10	Theta energy percentage	0.0217

IV. DISCUSSION

One of the most significant aspects of this study compared to the earlier works is the utilization of an extensive and diverse dataset. The proposed model is based on 15,324 trials from 48 subjects, which substantially aided the generalization. We explored temporal, spectral, and spectro-temporal domains to extract meaningful features from the EEG data. We also employed several machine learning algorithms to assess both linear and non-linear relationships, and all the outcomes were validated using 10 randomizations. All of these ingredients ensure the reliability of the model.

In our investigation, the Random Forest model outperformed other models, for both regression and classification. The performance difference between the Linear Regression and the Random Forest model indicates the inherent non-linearity in the relationship. Our channel selection method suggests that the left-back part of the brain plays the most vital role in this visual task. It makes sense, as most of the people are right-handed, and response using the right hand utilizes the left part of the brain. Also, our feature selection method demonstrates the eminence of theta and alpha band, which agrees to the present findings [10]. We believe our work will contribute to the further advancements of brain-computer interface design and biomedical signal processing.

REFERENCES

[1] A. F. Rabbi, K. Ivanca, A. V. Putnam, A. Musa, C. B. Thaden, and R. Fazel-Rezai, "Human performance evaluation based on EEG signal analysis: a prospective review," in *31st Annual International Conference of the IEEE Engineering in Medicine and Biology Society*, 2009, pp. 1879-1882.

[2] D. Wu, B. J. Lance, V. J. Lawhern, S. Gordon, T.-P. Jung, and C.-T. Lin, "EEG-Based User Reaction Time Estimation Using Riemannian Geometry Features," *IEEE Transactions on Neural Systems and Rehabilitation Engineering*, vol. 25(11), November 2017, pp. 2157–2168.

[3] A. Luo and P. Sajda, "Using Single-Trial EEG to Estimate the Timing of Target Onset During Rapid Serial Visual Presentation," in *28th Annual International Conference of the IEEE Engineering in Medicine and Biology Society*, 2006, pp. 79–82.

[4] K. Aboalayon, M. Faezipour,W. Almuhammadi, and S. Moslehpour, "Sleep Stage Classification Using EEG Signal Analysis: A Comprehensive Survey and New Investigation," *Entropy*, vol. 18(9), August 2016, p. 272.

[5] S. Charbonnier, L. Zoubek, S. Lesecq, and F. Chapotot, "Self-Evaluated Automatic Classifier as a Decision-Support Tool for Sleep/Wake Staging," *Computers in Biology and Medicine*, vol. 41(6), 2011, pp. 380–389.

[6] M. Radha, G. Garcia-Molina, M. Poel, and G. Tononi, "Comparison of Feature and Classifier Algorithms for Online Automatic Sleep Staging Based on a Single EEG Signal," in *36th Annual International Conference of the IEEE Engineering in Medicine and Biology Society*, 2014, pp. 1876–1880.

[7] K.A. Aboalayon and M. Faezipour, "Multi-Class SVM Based on Sleep Stage Identification Using EEG Signal," in *IEEE Healthcare Innovation Conference (HIC)*, 2014, pp. 181–184.

[8] L. Fraiwan, K. Lweesy, N. Khasawneh, H. Wenz, and H. Dickhaus, "Automated Sleep Stage Identification System Based on Time-Frequency Analysis of a Single EEG Channel and Random Forest Classifier," *Computer Methods and Programs in Biomedicine*, vol. 108(1), October 2012, pp. 10–19.

[9] H. Peng, F. Long, and C. Ding, "Feature Selection Based on Mutual Information: Criteria of Max-Dependency, Max-Relevance, and Min-Redundancy," *IEEE Trans. Pattern Analysis and Machine Intelligence*, Vol. 27, No. 8, 2005, pp 1226-1238.

[10] L. J. Trejo, K. Kubitz, R. Rosipal, R. L. Kochavi, and L. D. Montgomery, "EEG-Based Estimation and Classification of Mental Fatigue," *Psychology*, Vol.06, No.05, 2015, pp. 572-589.